Published in final edited form as:
Neuroscience. 2010 February 17; 165(4): 1519. doi:10.1016/j.neuroscience.2009.11.040.

Cell-type Specific Distribution of Chloride Transporters in the Rat Suprachiasmatic Nucleus

Michael A. Belenky[1,2], **Patricia J. Sollars**[3], **David B. Mount**[4], **Seth L. Alper**[5], **Yosef Yarom**[2], and **Gary E. Pickard**[3]

[1]Department of Cell and Developmental Biology, Hebrew University of Jerusalem, Jerusalem, 91904 Israel

[2]Department of Neurobiology, Institute of Life Sciences, Hebrew University of Jerusalem, Jerusalem, 91904 Israel

[3]Department of Veterinary and Biomedical Sciences, University of Nebraska, Lincoln, NE, USA 68583

[4]Renal Divisions, Brigham and Women's Hospital, Veterans Affairs Boston Healthcare System, Harvard Medical School, Boston, Massachusetts, USA 02115

[5] Molecular and Vascular Medicine Unit and Renal Division, Harvard Medical School, Boston, Massachusetts, USA 02215

Abstract

The suprachiasmatic nucleus (SCN) is a circadian oscillator and biological clock. Cell-to-cell communication is important for synchronization among SCN neuronal oscillators and the great majority of SCN neurons use γ-aminobutyric acid (GABA) as a neurotransmitter, the principal inhibitory neurotransmitter in the adult central nervous system. Acting via the ionotropic $GABA_A$ receptor, a chloride ion channel, GABA typically evokes inhibitory responses in neurons via Cl^- influx. Within the SCN GABA evokes both inhibitory and excitatory responses although the mechanism underlying GABA-evoked excitation in the SCN is unknown. GABA-evoked depolarization in immature neurons in several regions of the brain is a function of intracellular chloride concentration, regulated largely by the cation-chloride cotransporters NKCC1 (for chloride entry) and KCC1-4 (for chloride egress). It is well established that changes in the expression of the cation-chloride cotransporters through development determines the polarity of the response to GABA. To understand the mechanisms underlying GABA-evoked excitation in the SCN, we examined the SCN expression of cationchloride cotransporters. Previously we reported that the K^+/Cl^- cotransporter KCC2, a neuron-specific chloride extruder conferring GABA's more typical inhibitory effects, is expressed exclusively in vasoactive intestinal peptide (VIP) and gastrin-releasing peptide (GRP) neurons in the SCN. Here we report that the K^+/Cl^- cotransporter isoforms KCC4 and KCC3 are expressed solely in vasopressin (VP) neurons in the SCN whereas KCC1 is expressed in VIP neurons, similar to KCC2. NKCC1 is expressed in VIP, GRP and VP neurons in the SCN as is WNK3, a chloride-sensitive neuron-specific serine-threonine kinase which modulates intracellular chloride concentration via opposing actions on NKCC and KCC cotransporters. The

Corresponding author: Gary E. Pickard, Ph.D. Department Veterinary and Biomedical sciences University of Nebraska Lincoln, NE 68583 Phone 402 472-8558 Fax 402 472-9690 gpickard2@unl.edu.

heterogeneous distribution of cation-chloride cotransporters in the SCN suggests that Cl^- levels are differentially regulated within VIP/GRP and VP neurons. We suggest that GABA's excitatory action is more likely to be evoked in VP neurons that express KCC4.

Keywords

circadian rhythms; GABA; KCC2; KCC3; KCC4; NKCC1; WNK3

The hypothalamic suprachiasmatic nucleus (SCN) is a circadian oscillator which functions as a biological clock (Hastings et al. 2003; Herzog, 2007; Pickard and Sollars, 2008). The SCN generates an endogenous rhythm in neural activity in the absence of external temporal cues with action potential firing rate high during the subjective day and low during the subjective night (Brown and Piggins, 2007). Many SCN neurons function as autonomous oscillators and cell-to-cell communication is responsible for synchronization among neuronal oscillators and between sub-regions within the SCN (Welsh et al. 1995; Yamaguchi et al. 2003; Quintero et al. 2003; Herzog et al. 2004; Albus et al. 2005; Aton and Herzog, 2005). The majority of SCN neurons contain γaminobutyric acid (GABA) and express glutamate decarboxylase, a key enzyme of GABA synthesis (Moore and Speh, 1993; Belenky et al. 1996, 2008; Castel and Morris, 2000). Most synaptic terminals within the mammalian SCN are GABAergic (van den Pol, 1986), SCN neurons are interconnected by GABAergic synapses (Strecker et al. 1997), and both $GABA_A$ and $GABA_B$ receptors are widely, although unevenly, distributed throughout the SCN (Gao et al. 1995; Belenky et al. 2003, 2008). GABA appears to play an important role in intra-SCN network activity and synchronization of firing rhythms among SCN neurons (Liu and Reppert, 2000; Shirakawa et al. 2000; Albus et al., 2005) although it has also been reported that GABA signaling is not required for synchronization among SCN neurons (Aton et al. 2006).

Although GABA is typically considered an inhibitory neurotransmitter in the adult nervous system, GABA has been reported to evoke excitatory responses in the SCN. Wagner and colleagues (1997) first reported a day/night difference in GABA's action in the SCN with GABA decreasing firing frequency during the subjective night but increasing firing frequency during the subjective day. Whereas some investigators have reported only inhibitory effects of GABA in the SCN at all phases of the circadian cycle (Gribkoff et al. 1999; 2003), others have reported nocturnal excitatory effects of GABA (De Jeu and Pennartz, 2002). Albus and co-workers (2005) reported excitatory responses to GABA in the SCN but with a much higher incidence of GABA-evoked excitation in the dorsal as compared to the ventral SCN and these responses were more evident during the late day/early night. In a recent study by Choi and colleagues (2008), most GABA-evoked responses observed in the SCN were inhibitory but some GABA-mediated excitation was observed in both the dorsal and ventral SCN irrespective of the time of day. However, GABA-evoked excitatory responses were most commonly observed during the night in the dorsal SCN region (Choi et al. 2008). There is growing consensus that GABA can evoke excitatory responses in mature SCN neurons, however it remains unclear if these responses are restricted to particular phases of the circadian cycle and/or to particular cell types or sub-regions of the nucleus.

The cellular mechanisms underlying GABA-evoked excitation in the SCN are unknown. It is well documented that GABA acts as an excitatory neurotransmitter early in the development of the central nervous system (Payne et al. 2003; Ben-Ari et al. 2007). The ionotropic $GABA_A$ receptor is a Cl^- channel that opens upon GABA binding. In immature neurons, $GABA_A$ receptor-mediated responses are depolarizing and facilitate the generation of Na^+ and Ca^{2+} currents whereas later during development and in mature neurons, $GABA_A$ receptor-mediated responses are hyperpolarizing. The shift in GABAergic responses during

development is related to the expression and function of cation-chloride cotransporters (Rivera et al., 1999).

Electroneutral in nature, cation-chloride cotransporters do not generate any current but rather contribute to the inwardly or outwardly directed net flux of ions generated by gradients that are set by active transporters such as Na^+/K^+-ATPase. Thus the neuronal K^+ gradient is employed by the K^+/Cl^- cotransporter (KCC) to extrude Cl^- from the cell whereas the $Na^+/K^+/2Cl^-$ cotransporters (NKCC) use the neuronal Na^+ gradient to increase intracellular Cl^- concentration ($[Cl^-]_i$). During early postnatal development, expression of NKCC1 is high, raising $[Cl^-]_i$. As development proceeds, KCC2 expression increases, lowering intracellular Cl^- resulting in the characteristic inhibitory responses to GABA (Rivera et al. 1999; Payne et al. 2003).

It has been suggested that $[Cl^-]_i$ may be dynamically regulated within the SCN (Wagner et al. 1997, 2001) and a circadian rhythm in $[Cl^-]_i$ has been reported in acutely dissociated SCN neurons (Shimura et al. 2002). The role of cation-chloride cotransporters in regulating $[Cl^-]_i$ in the mammalian SCN has only recently begun to be examined. Using in situ hybridization, mRNA expression for two of the four known isoforms of the K^+/Cl^- cotransporter, KCC1 and KCC2 were localized to the ventrolateral SCN (Kanaka et al. 2001). KCC2 is neuron specific and is thought to be the main chloride extruder in the nervous system whereas KCC1 is widely expressed in different tissues and is considered to be a “housekeeping” transporter (Hebert et al. 2004). KCC2 protein was subsequently shown to be expressed exclusively in vasoactive intestinal peptide (VIP) and gastrin-releasing peptide (GRP) neurons located in the ventral and ventrolateral SCN; no KCC2 was observed in neurons expressing vasopressin (VP) (Belenky et al. 2008). KCC4 mRNA has also been described in the SCN whereas the same study found no evidence for KCC3 expression in the SCN (Le Rouzic et al. 2006).

In the present study using immunocytochemical procedures at both the light and electron microscopic level of examination, we describe the distribution of KCC4, KCC3 and KCC1 in the SCN. In addition we examine the distribution of NKCC1, a chloride cotransporter responsible for Cl^- influx, and WNK3, a chloride-sensitive protein kinase that modulates cellular Cl^- flux by altering the phosphorylation state of cation-chloride cotransporters (Kahle et al. 2008). To define more precisely the cellular localization of these proteins within the SCN, double-label immunocytochemical experiments were conducted to determine whether the cotransporters were expressed in a cell-type specific manner in association with VIP, GRP, or VP neurons.

EXPERIMENTAL PROCEDURES

Animals and tissue preparation

Thirty two adult male rats of the Sprague-Dawley strain (Harlan Israel, Jerusalem) were used for light and electron microscopic immunocytochemical analysis of chloride transporters in the SCN. Animals were housed in cages with food and water available *ad libitum* and maintained under a 12 h light:12 h dark cycle with lights on at 07:00 h. To analyze transporter expression at different stages of the light/dark cycle, a group of rats (n= 5) was maintained under an inverted day/night cycle with lights on at 19:00 h; all animals were killed between 11:00 and 13:00 h. All procedures used in the study adhered to guidelines approved by the Hebrew University of Jerusalem Animal Care and Use Committee and conform to National Institutes of Health (USA) guidelines. All possible efforts were made to minimize animal suffering and the number of animals used.

Prior to fixation, rats were deeply anaesthetized with pentobarbital (40 mg/kg) ip. After opening the thorax, approximately 100 μl of heparin (5000 IU/ml; Choay, Paris, France) were injected

into the left cardiac ventricle, followed by transcardiac perfusion with phosphate buffered saline (PBS) (0.1 M phosphate buffer (PB) containing 0.9% sodium chloride; pH 7.4) and then by perfusion with 300 ml of freshly prepared fixative containing either 4% paraformaldehyde (PFA) or 4% PFA solution enriched with 0.25% glutaraldehyde (both from Electron Microscopy Sciences, Fort Washington, PA) in 0.1 M PB. Brains were dissected, trimmed and stored in the same fixative for an additional four-five hours at room temperature (RT). The brains were serially sectioned in the coronal plane with a Vibratome (Technical Products International, St. Louis, MO) at 30 or 50 μm for light and electron microscopy, respectively, and sections through the SCN region were collected in ice-cold PBS.

Colchicine injections—To increase accumulation of neuropeptides and chloride cotransporter proteins within SCN cells, rats (n=9) were anaesthetized with sodium pentobarbital (40 mg/kg) ip, placed into a BenchMark Angle One stereotaxic instrument (myNeuroLab.com, St. Louis, MO), and prepared for aseptic surgery. A metal cannula connected via a plastic tube to a 10 μl Hamilton syringe (Hamilton, Reno, NV) was used to inject 10 μl of colchicine solution (10 μg/μl in 0.9 % saline; Sigma, St. Louis, MO) into the lateral ventricle (stereotaxic coordinates relative to bregma with skull flat: anteroposterior, −1.2 mm; medio-lateral, +1.4 mm; dorsoventral, −3.4 mm from the top of the skull) and animals were killed 24 to 48 hours later.

Immunocytochemistry

Antibody sources—A variety of antibodies was used in this study to detect chloride cotransporters and associated molecules and to determine the peptidergic nature of the neurons in which they were expressed. A compilation of antibodies used is presented in Table 1.

Light microscopic immunocytochemistry—For light microscopic immunoperoxidase and immunofluorescence labeling, free-floating 30 μm thick vibratome sections were pre-treated with 0.3% H_2O_2 in PBS (15 min; for sections intended for immunoperoxidase labeling and tyramide signal amplification only) to inactivate endogeneous peroxidases. In the case of antibodies against NKCC1, the samples were then treated with 1% SDS (sodium dodecyl sulfate) in PBS containing 8% 2-mercaptoethanol (5 min, RT). For KCC3 antigen retrieval, vibratome sections were treated with 20 μg/ml proteinase K in PBS containing 1% BSA for 4 min at 37° C and then after washes in PBS, with SDS/mercaptoethanol mixture as described above (Person et al. 2001). Finally, after thorough washing in PBS, the sections were incubated in a blocking solution (5% normal goat or donkey serum, 2% egg albumin, 0.5% glycine, 0.5% lysine in PBS, 1h at RT) followed with a primary antibody diluted in PBS containing 1% normal goat or donkey serum and 0.5% egg albumin. Subsequently, 0.3% Triton X-100 was added both to the blocking solution and the primary antibody solution, and the samples were incubated for 24-48 h at RT. After thorough washing in PBS the samples were incubated in for 90 min at RT in an appropriate secondary antibody: either biotinylated IgG (1:500; Vector Laboratories, Burlingame, CA) or IgG conjugated with AlexaFluor 488 or AlexaFluor 594 (1:500; Molecular Probes, Eugene, OR), or Cy2 and Cy3 (1:300, Jackson ImmunoResearch Laboratory, West Grove, PA). In the case of immunoperoxidase labeling, this step was followed with a treatment with ABC solution (ABC *Elite* kit; Vector Laboratories) and 3,3′-diaminobenzidine tetrahydrochloride (DAB, 5mg/20 ml PBS with 4 μl of H_2O_2) as the chromogen.

In many cases, the intensity of fluorescent signal was increased using Renaissance TSA fluorescence tyramide signal amplification kit (NEL 704; Perkin Elmer, Boston, MA). Briefly, after thorough washing in PBS following incubation with the primary antibody, the sections were incubated in an appropriate biotin-conjugated secondary antibody (either from Vector Laboratories, Burlingame, CA, 1:600 or from Jackson ImmunoResearch Laboratory, 1:1000),

then in streptavidin conjugated to horseradish peroxidase (HRP, 1:100) and finally in tyramide amplification reagent conjugated to Cy3 (up to 10 minutes, RT).

For double immunostaining, free-floating sections through the SCN were incubated in a cocktail of the primary antibodies, each raised in a different species. Secondary antibodies used in double-immunolabeling experiments were always generated in the same species, either affinity-purified donkey or affinity-purified goat antibodies which exhibit minimal cross-reaction to serum proteins of several species. Additionally, the absence of cross-reactivity between the secondary antibodies was verified by omitting one of the primary antibodies. Secondary antibodies used in this case were conjugated to either AlexaFluor 488 or AlexaFluor 594. In many cases one of immunoreactivities was subjected to signal amplification using a tyramide kit as described above. It proved important to carry out amplification steps (streptavidin-HRP and tyramide-Cy3 incubations) at the end of the staining protocol to exclude problems that may have arisen with penetration into the sections of the second secondary antibody used for "direct" labeling. In rare cases when both primary antibodies were raised in the same species (e.g. KCC2/KCC4 immunostainings), the method of Shindler and Roth (1996) was applied in which sequential labeling of the samples is performed; one of the primary antibodies is used at a dilution approximately ten times higher than is normally used for immunodetection followed with tyramide signal amplification, and then the second antigen was labeled using a conventional immunofluorescence staining protocol with second primary antibody diluted normally. The following steps were used: 1) incubation in the first primary antibody (anti-KCC2 1:7500, overnight, RT), 2) biotinylated goat anti-rabbit IgG (2 h, RT); 3) incubation in the second primary antibody (anti-KCC4, 1: 1000, overnight, RT); 4) goat-anti rabbit IgG conjugated with AlexaFluor 488 (1:1000, 2 h); 5) streptavidin-HRP (1:100) and goat-anti rabbit IgG conjugated with AlexaFluor 488 (45 min); 6) tyramide-Cy3 (1:100, up to 10 min). The samples were mounted on subbed slides and those intended for fluorescence microscopy were coverslipped with Vectashield mounting medium (Vector Laboratories).

Pre-embedding HRP immunocytochemistry for electron microscopy—

Immunolabeling at the electron microscopic level was performed using free-floating sections according to the protocol described earlier (Belenky et al., 2008). Briefly, after mild treatment with H_2O_2 (0.015% in PBS, 15 min; only for samples intended for immunoperoxidase labeling and tyramide signal amplification), sections were cryoprotected with a sucrose/glycerol mixture. They were then frozen in liquid nitrogen-cooled isopentane (2-methylbutane, Sigma, St. Louis, MO) and then in liquid nitrogen (60 sec each) and thawed in PBS. The samples were then incubated in a blocking solution (1h), primary antibody (24 h at RT) and then subjected to a routine immunoperoxidase labeling procedure as described earlier while the amount of Triton X-100 both in the blocking solution and the primary antibody was reduced to a maximum of 0.03%. After thorough washing in PBS the samples were incubated for 2 h at RT in an appropriate biotinylated secondary antibody (1:500; Vector Laboratories, Burlingame, CA). This step was followed with a treatment with ABC solution (ABC *Elite* kit; Vector Laboratories) and DAB (5mg/20 ml PBS with 4 μl of H_2O_2) as the chromogen. In some cases (e.g. NKCC1 or WNK3 immunodetection), tyramide signal amplification was included in the standard electron microscopic protocol: after the incubation in ABC solution, the vibratome sections were treated for 10 min at RT with tyramide conjugated to biotin and then again with ABC reagent and finally with DAB. In many cases the HRP reaction product, visualized using DAB as the chromogen, was further enhanced and substituted with silver/gold particles (see Belenky et al., 2008 for details). Briefly, immunostained sections were thoroughly washed in 2% sodium acetate solution and then incubated for 15 min at 60° C in a solution containing 2.6% hexamethylene tetramine, 0.2% silver nitrate, and 0.2% borax. After thorough rinsing, the sections were treated with 0.05% $HAuCl_4$ solution for 5 min at room temperature and after further washing in sodium acetate, were incubated in a 1% $Na_2S_2O_3$ solution to remove the unbound silver ions.

Pre-embedding immunogold-silver labeling—This technique was used for detection of KCC2, KCC4 and WNK3 immunoreactivities as well as VP and VIP in the SCN. Vibratome cut sections were incubated in the primary antibodies as described above. After rinsing in PBS, the sections were placed in a blocking solution containing 0.5% BSA and 0.1% cold water fish gelatin in PBS (15 min, at RT) and then transferred to donkey anti-rabbit IgG or anti-mouse IgG Fa,b' fragments or goat-anti guinea pig IgG all conjugated to UltraSmall colloidal gold (Aurion, Wageningen, The Netherlands) diluted 1:90 with BSA/gelatin/PBS (6 h at room temperature or overnight at 4° C). Gold particles were enlarged for microscopic examination with the Aurion R-Gent SF-EM silver enhancement kit (90 min at 20° C). Finally, the samples were postfixed in 2.5% glutaraldehyde in PB, thoroughly washed with PBS and then with sodium acetate solution and then were toned with a 0.05% aqueous gold chloride solution (10 min at room temperature under dim light), treated with 1% sodium thiosulfate solution (10 min), and thoroughly washed in sodium acetate solution and then in PBS. In the case of double labeling with involvement of both pre-embedding immunoperoxidase staining and pre-embedding immunogold labeling, all steps of immunoperoxidase procedure were carried out first to exclude sedimentation of HRP reaction product (DAB material) on silver particles.

All SCN samples were then postfixed in a mixture of 1% osmium tetroxide and 1.5% potassium ferricyanide in 0.1M cacodylate buffer pH 7.0, dehydrated in ascending concentrations of ethanol and flat-embedded between two sheets of Aclar film (Ted Pella, Redding, CA) in EM-BED812 (Electron Microscopy Sciences). Ultrathin sections prepared with a Reichert Ultracut were lightly stained with uranyl acetate and lead citrate.

Post-embedding immunogold labeling—Immunogold staining was used to visualize GABA immunoreactivity in the SCN samples embedded in epoxy resin and stained previously for WNK3 immunoreactivity. The staining procedure has been described previously (Belenky et al., 2008). Briefly, ultrathin sections collected on nickel grids were incubated in saturated aqueous sodium *m*-periodate (45 min), thoroughly washed in Tris buffered saline (TBS, pH 7.4) containing 0.85% NaCl, 0.5% BSA, 0.13% sodium azide and 0.5% Tween20, and then placed in 2% egg albumin in TBS as blocker. In some cases, to exclude “washing out” of silver/gold particles after the preceding pre-embedding staining (for WNK3), pretreatment with *m*-periodate was omitted from the protocol (Renno, 2001). Then the sections were incubated in the primary antibody diluted in TBS containing 0.5% egg albumin for at least 5 hr at room temperature or overnight at 4° C, followed by goat or donkey anti-rabbit IgG conjugated to 12 nm gold particles (1:10; 90 min, RT; Jackson ImmunoResearch Laboratory). Finally, the sections were postfixed in 2% aqueous glutaraldehyde (10 min) and contrasted as described above. Specificity of immunostaining was detected using samples incubated in pre-adsorbed antibodies (10-40 μg/ml; 48 h at 4° C) or in the vehicle with omission of the primary antibodies. Non-specific binding was negligible in all cases.

The specificity of immunolabeling for chloride transporters and WNK3 was verified at both the light and electron microscopic levels by either increasing dilutions of the primary antibodies, by omitting the primary antibody, or by incubation in the primary antiserum preadsorbed with an excess of the specific peptide used as immunogen for raising the primary antibody (10-40 μg/ml, 48 h at 4°C). These experiments led to complete elimination of the immunostaining in all cases.

Microscopy and analysis

Light microscopic images were captured using an Axioskop-2 microscope (Zeiss, Oberkochen, Germany) equipped with a cooled KX-85 CCD camera (Apogee Instruments, Tucson, AZ). Immunofluorescence material was then examined using an Olympus FluoView 1000 confocal microscope equipped with an argon ion laser (excitation at 488 nm) and a He/Ne laser

(excitation at 533 nm). Sequential 1 μm optical sections were collected at 505-525 nm and 560-620 nm for green and red channels, respectively. They were stored as 512- × 512-pixel or 1024- × 1024-pixel images. Unambiguous identification of double-fluorescent neurons was achieved by analysis of several confocal planes through the same structure. Digital images were pseudo-colored and enhanced for brightness/contrast using Image-Pro Plus software, version 5.1 (Media Cybernetics, Silver Spring, MD). Confocal images are presented either as a stack of optical sections or more often as single optical sections.

Ultrathin sections were viewed in Tecnai-12 (Philips) electron microscope equipped with a MegaView II CCD camera and AnalySIS software version 3.0 (Soft Imaging System, Munster, Germany). All photomicrographs were unaltered except for brightness/contrast enhancement.

RESULTS

KCC4 is associated with VP neurons in the SCN

Robust labeling for KCC4, one of the four K^+/Cl^- cotransporter isoforms responsible for chloride extrusion from cells, was observed in the SCN using a well-characterized rabbit polyclonal antibody (Karadsheh et al. 2004) and confocal microscopy. KCC4 staining appeared relatively more intense in SCN neuronal perikarya compared to processes intermingled amongst the labeled perikarya (Fig. 1a). Double-labeling of SCN sections with KCC4 and VP antibodies revealed that throughout the SCN KCC4 immunostaining is associated exclusively with VP-containing profiles (Fig. 1e). In the central and especially more caudal aspects of the SCN, some VP cells are located in the ventral area of the nucleus outside of the dorsomedial region considered to be the primary site of VP neurons, and occasionally VP neurons are observed in close proximity to the optic chiasm. Nevertheless, these VP cells were also intensely labeled for KCC4; all VP cells were KCC4 positive indicating that expression of KCC4 is neuron-type specific in the SCN (Fig. 1e). Although the extent of co-localization appears variable in the 1 μm optical sections presented in Figure 1e, all VP cells were KCC4 positive. No co-localization was detected when SCN sections were double stained with antibodies against KCC4 and either VIP or GRP (data not shown). Taken together with our previous finding that the neuron-specific K^+/Cl^- isoform KCC2 is associated only with VIP and GRP neurons in the SCN (Belenky et al. 2008), the data suggest that KCC2 and KCC4 are differentially expressed between the two major SCN neuropeptide populations (i.e., VIP/GRP and VP).

To test directly that KCC4 and KCC2 are differentially localized in SCN neurons, sections were double-labeled for KCC4 and KCC2. No co-localization was observed in these experiments confirming that the two K^+/Cl^- isoforms are associated with different structures in the SCN (Figs. 1a-d). Thus, it appears that KCC2 is found exclusively in VIP and GRP neurons whereas KCC4 is expressed only in VP neurons in the SCN.

At the electron microscopic level (using pre-embedding immunoperoxidase labeling followed by silver/gold substitution or pre-embedding immunogold staining), labeling for the KCC4 cotransporter was observed predominately, although not exclusively, in the dorsomedial SCN region, in agreement with the light microscopic observations. In the SCN, KCC4 immunolabeling was detected in numerous perikarya and thin dendritic profiles whereas no axonal structures were labeled. Immunoreaction product was associated with the cisternae of rough endoplasmic reticulum and occasional labeling was also detected along the plasma membrane (Figs. 2a,b). The co-expression of VP and KCC4 observed using confocal microscopy (Fig.1e) was confirmed at the electron microscopic (data not shown). Thus, in the rat SCN, KCC4 is expressed only in VP neurons and all VP neurons express KCC4.

KCC3 is associated with VP neurons in the SCN

To determine the pattern of KCC3 expression in the SCN, we used a well-characterized KCC3 affinity-purified antibody in combination with an antigen retrieval procedure based on proteinase K (Pearson et al. 2001). This approach revealed unambiguous KCC3 immunoreactivity in the SCN with the staining predominately within perikarya of SCN neurons; immunopositive neuronal processes were observed to a much lesser extent (Figs. 3a,d). Double-label experiments with antibodies against KCC3 and VP revealed distinct expression of both antigens in the same cells (Figs. 3a-f). In addition there was clear KCC3 labeling of ependymal cells lining the surface of the third ventricle as well as some neuronal perikarya and fiber profiles located between the ependymal layer and the SCN proper. No electron microscopic immunocytochemical analysis was performed for KCC3 due to incompatibility of the KCC3 antigen retrieval procedure with ultrastructural preservation of the tissue.

KCC1 expression is similar to that of KCC2 in the SCN

Immunofluorescence confocal microscopic analysis using a well-characterized antibody directed against a C-terminus fragment of KCC1 (Su et al. 1999; Roussa et al. 2002) revealed a very distinct pattern of immunolabeling in the SCN (Fig. 1f). In the ventral region, KCC1 immunolabeling was extremely prominent whereas the dorsal SCN exhibited a low level of immunostaining with only individual KCC1-immunoreactive fibers noted that appeared to traverse the region. Double staining experiments revealed no expression of KCC1 in VP neurons whereas KCC1 was expressed in VIP positive profiles. Additionally, KCC1 immunoreactivity was detected in the ependymal cells of the third ventricle as well as in structures located between the SCN proper and the ependymal cell layer lining the third ventricle (data not shown). Overall the expression of KCC1 in the SCN is very similar to that of KCC2 (Fig. 1b, c) with the exception of ependymal cell involvement characteristic only of KCC1.

NKCC1 is expressed in neurons throughout the SCN

The distribution of the $Na^+/K^+/2Cl^-$ cotransporter NKCC1 in the SCN was examined with two different antibodies. The general pattern of labeling observed in the SCN was similar with both antibodies although some differences were noted; the rabbit antibody (code NKCC11a, Alpha Diagnostic) showed labeling primarily of neuronal perikarya whereas the antibody produced in chicken, (code ab37792, Abcam) stained both cells and fiber profiles equally well.

At the light microscopic level, with pre-embedding immunoperoxidase labeling using the rabbit NKCC1 antibody, immunoreactivity was more intense in dorsal and dorsomedial areas of the nucleus, regions of the SCN normally occupied by VP neurons. NKCC1 labeling of VP neurons was subsequently confirmed by examination of images captured from SCN sections stained first for VP using an immunofluorescence approach (Fig. 4a) and then for NKCC1 using immunoperoxidase labeling (Fig. 4b). When the chicken NKCC1 antibody was used in a double-label paradigm and analyzed by confocal immunofluorescence microscopy, NKCC1 label observed in the SCN was principally associated with perikarya of VP neurons and to a much lesser extent with dendrite-like profiles (Figs. 5a-c). In the ventral SCN the predominately perikaryal expression of NKCC1 that is characteristic of VP neurons, was less apparent; NKCC1 immunostaining in the ventral SCN was more often observed as numerous discrete puncta or fiber-like profiles (Fig. 6). High magnification confocal images captured from SCN sections double-stained for NKCC1 and VP, VIP or GRP showed that the chloride cotransporter was expressed in neuropeptide immunopositive neurons (Figs. 5c-e; 7c). However, because co-expression of the neuropeptides and NKCC1 was evaluated one neuropeptide at a time, there were always NKCC1 immunopositive cells that were not labeled with the peptide being examined. Colchicine pre-treatment of the animals resulted in an

increase in the intensity of immunostaining both for the chloride cotransporter and the neuropeptides but colchicine treatment did not change the overall pattern of immunolabeling. NKCC1 immunoreactivity was also detected in the ependyma lining the third ventricle as well in the region directly adjacent to the ventricle known to be occupied primarily with numerous fiber projections and few neuronal perikarya. Thus, NKCC1 is expressed throughout the SCN and is co-localized with at least VP, VIP, and GRP neurons in the SCN; no additional neuropeptides were examined

NKCC1 alone is responsible for regulating Cl^- influx in neurons and thus might play a pivotal role in determining the action of GABA in the SCN at different phases of the circadian cycle. Labeling for NKCC1 in the SCN from animals sacrificed 5 h after lights on (Zeitger Time [ZT] 5) (≈ middle of the day) vs animals sacrificed at ZT 17 (≈ middle of the night) did not reveal robust differences in staining in the SCN (Figs. 6a,b).

At the electron microscopic level (using pre-embedding immunoperoxidase labeling followed by silver/gold substitution), clear labeling for the NKCC1 chloride cotransporter was observed throughout the SCN. NKCC1 immunolabeling was detected in the cell somata in association with the cisternae of rough endoplasmic reticulum and clear labeling was also detected in the soma and in dendritic profiles along the plasma membrane (Figs. 7a,c). Double-labeling revealed that NKCC1 was co-localized with KCC4 in SCN neurons (Figs. 2a,b). In addition, the NKCC1 chloride cotransporter was detected in the ependymal cells lining the bottom of the third ventricle (Fig. 7b).

WNK3 kinase is expressed in the SCN

In this next set of experiments we examined the SCN for WNK3, a chloride-sensitive serine-threonine kinase implicated in the regulation of cellular Cl^- flux and GABA-induced depolarization (Kahle et al. 2005, 2008). WNK3 immunolabeling was noted throughout the SCN in neuronal perikarya and in dendrite-like profiles (Fig. 8a). The pattern of labeling observed was similar with the two different commercial antibodies used. A double staining procedure utilizing a combination of anti-WNK3 antibody with VP and VIP antibodies revealed that this kinase is co-expressed in both types of peptidergic neuron in the SCN (Figs. 8b-g). As in the case of the chloride cotransporters examined, colchicine injection into the lateral ventricle of experimental animals did not change the pattern of WNK3 expression but simply increased the intensity of labeling. In addition to the staining of neuronal profiles within the SCN proper, labeling for WNK3 was also noted in the ependyma of the third ventricle (not shown).

At the electron microscopic level, labeling for WNK3 was observed in perikarya and in dendritic profiles of SCN neurons in agreement with the light microscopic analysis. In the cell somata, WNK3 immunoreaction product was detected over the cisternae of rough endoplasmic reticulum, over the numerous dense core vesicles and also near the plasma membrane (Fig. 9a). In dendritic profiles the labeling was detected most often in the vicinity of the plasma membrane especially in the postsynaptic region of synapses (Fig. 9b,c). Double labeling employing pre-embedding immunoperoxidase staining with silver/gold substitution for WNK3 and post-embedding immunogold staining for GABA revealed that most of the synapses that WNK3 was associated with were GABAergic (Fig. 9c). Ultrastructural investigation of SCN sections double stained with antibodies against WNK3 and NKCC1 revealed that both antigens are co-localized in the vast majority of analyzed cells in the SCN (not shown).

DISCUSSION

K^+/Cl^- Cotransporters in the SCN

Potassium/chloride cotransporters convey Cl^- out of cells and thus play a major role in maintaining low neuronal intracellular Cl^- levels. Four K-Cl isoforms have been identified and we provide evidence that their expression is neuron-type specific in the SCN: KCC4 and KCC3 are expressed only in neurons also containing VP whereas KCC2 and KCC1 are found exclusively in VIP and GRP neurons. The KCC3 isoform of the K^+/Cl^- cotransporters has not previously been described in the SCN. Le Rouzic and colleagues (2006) failed to detect KCC3 expression in the rat hypothalamus using antisense riboprobes against the KCC3a splice variant, which is abundantly expressed in brain (Pearson et al. 2001). A hybridization signal for KCC4 mRNA has been described for the SCN although the peptidergic signature of neurons expressing KCC4 was not specified (Le Rouzic et al. 2006). We have previously reported that KCC2 is expressed in the SCN in a neuron-type specific manner in VIP and GRP neurons (Belenky et al. 2008). A low level of KCC1 mRNA has been reported in the SCN in the ventrolateral part of the nucleus, a region normally occupied by VIP and GRP cells, although the neurochemical identity of the cells expressing KCC1 was not determined; no KCC1 signal was noted in the dorsomedial SCN sub-region (Kanaka et al. 2001). We extend the findings of Kanaka and colleagues (2001) by demonstrating that KCC1 is expressed in VIP cells in the SCN.

Our current results taken together with our previous findings and those of other investigators provide unambiguous evidence for the differential expression of the K^+/Cl^- cotransporters in the SCN. KCC2 and KCC1 are expressed in VIP/GRP neurons whereas KCC4 and KCC3 are found in VP neurons. Based on the robustness of immunostaining for protein or hybridization signal for message, KCC2 and KCC4 appear to be the dominant K^+/Cl^- isoforms in VIP/GRP and VP neurons, respectively. In other regions of the central nervous system, KCC2 and KCC4 are differentially expressed. In large motor neurons of the spinal cord and brainstem, no KCC4 was detected in the spinal motor neurons that express KCC2 (Hubner et al. 2001) whereas large motor neurons in the brainstem that contribute to the cranial nerves show strong KCC4 immunoreactivity (Karadsheh et al. 2004). The differential expression of K^+/Cl^- cotransporters in functionally similar sets of neurons suggests that Cl^- flux may be regulated differently perhaps to modulate the GABAergic input to these cells.

It may be informative to consider the distribution of the various K^+/Cl^- cotransporters along with the expression of GABA and GABA associated receptors (ionotropic $GABA_A$ receptors and metabotropic $GABA_B$ receptors) in the SCN. KCC2 and KCC1 are characteristic of VIP and GRP neurons in the SCN, cells that have a high density of GABA innervation (Belenky et al. 2008), a high expression of $GABA_A$ receptors (Gao et al.1995; Belenky et al. 2003) and a lack of or low expression of $GABA_B$ receptors (Belenky et al. 2008). Conversely, KCC4 and KCC3 cotransporters in the SCN are characteristic of VP neurons, cells that have a lower density of GABA innervation and $GABA_A$ receptors but a greater number of $GABA_B$ receptors (Belenky et al. 2008).

In addition to the cell-type specific localization for KCC2 and KCC4 in the SCN, the subcellular distribution of these K^+/Cl^- cotransporters is also different in VIP and VP cells. In VIP cells, KCC2 was observed more often in dendritic profiles (Belenky et al. 2008) whereas KCC4 is more often associated with the plasma membrane of the VP neuronal soma (current study). The functional significance of the bias for KCC2 dendritic vs KCC4 somal localization in SCN neurons is presently unknown. However, in the substantia nigra KCC2 is also expressed in a cell-type specific manner being found in GABAergic but not dopaminergic neurons (Gulácsi et al. 2003). In GABAergic neurons in the substantia nigra KCC2 is preferentially localized in the dendritic plasma membrane at the periphery of synapses at the postsynaptic site where the

major Cl^- load is generated (Gulácsi et al. 2003). Subcellular localization of NKCC1 to the axon initial segment is responsible for the GABA-evoked depolarization of axo-axonic input to cortical principal neurons (Khirug et al. 2008) whereas dendritic compartmentalization of NKCC2 and KCC2 to the proximal and distal dendrites of starburst amacrine cells in the retina underlies GABA-evoked depolarization and hyperpolarization, respectively (Gavrikov et al. 2006). The prominent dendritic localization of KCC2 in VIP (and GRP) neurons in the SCN may provide for a more efficient Cl^- removal and thus a greater probability that GABA will evoke an inhibitory response. The cell-specific expression of K^+/Cl^- isoforms in the SCN coupled with their different subcellular distribution suggests that Cl^- flux might be regulated differently in these two populations of SCN neurons. As will be discussed below, these observations may provide a coherent view on the ionic mechanisms regulating GABA-evoked excitation in the SCN.

The K^+/Cl^- cotransporters can be parsed into two phylogenic subgroups; KCC2 is paired with KCC4 whereas KCC1 is more homologous to KCC3 (Mercado et al. 2000; Hebert et al. 2004). KCC2 is a neuronal specific isoform whereas the other three isoforms are widely distributed (Karadsheh et al. 2001). The KCC2 isoform is also unique in that it mediates constitutive K^+/Cl^- cotransport under isotonic conditions whereas the other three K-Cl isoforms exhibit no apparent isotonic activity (Mercado et al. 2006). Moreover, KCC2 exhibits a much higher cation affinity than the other three K^+/Cl^- cotransporters (Hebert et al. 2004). When KCC1 and KCC4 were compared as representatives of each subgroup, clear functional, kinetic, and pharmacological differences were revealed when analyzed after expression in *Xenopus* oocytes, (Mercado et al. 2000). These differences may have important physiological implications particularly with regard to cellular volume regulation in non-neuronal tissues. It remains to be determined exactly how the functional differences between subtypes of K^+/Cl^- cotransporters translate into variations of ion flux regulation in neurons. It is however clear that deficiency of KCC3 and KCC4 can impact intracellular $[Cl^-]$ in neurons and epithelial cells, respectively (Boettger et al. 2002, 2003).

NKCC1 Cotransporter in the SCN

The neuronal transmembrane Cl^- gradient is maintained by a combination of Cl^- efflux via the K^+/Cl^- cotransporters and by Cl^- influx regulated by the $Na^+/K^+/2Cl^-$ cotransporter NKCC1 (Payne et al. 2003). In the current study NKCC1 was observed to be distributed throughout the SCN in association with VIP, GRP and VP neurons in agreement with Western blot analysis indicating NKCC1 protein in both the ventral and dorsal regions of the SCN (Choi et al. 2008). A functional role for NKCC1 in the regulation of $[Cl^-]_i$ in SCN neurons comes from pharmacological experiments employing the NKCC1 antagonist bumetanide; after bumetanide application the reversal potential of evoked EPSPs in SCN neurons shifted significantly to a more hyperpolarized potential (Choi et al. 2008). Choi and colleagues (2008) also report a two-fold increase in NKCC1 protein in the dorsal SCN at night (ZT 16) vs the day (ZT 4) determined from Western blot analysis of SCN sub-regions; our morphological analysis did not reveal robust differences in NKCC1 immunostaining at ZT 17 compared to ZT 5.

GABA-evoked Excitation in the SCN

$GABA_A$ receptor activation in mature neurons typically generates a net influx of Cl^- resulting in hyperpolarization and inhibition. In immature neurons GABA depolarizes and evokes excitation by gating Cl^- efflux (Kaila, 1994). The level of expression of NKCC1 and KCC2 in immature neurons appears to determine $[Cl^-]_i$. Rivera and colleagues (1999) reported that as development proceeds in the hippocampus, KCC2 is up-regulated resulting in a reduction in $[Cl^-]_i$ and a reversal of GABA-evoked depolarization to GABA-evoked hyperpolarization. Thus as the central nervous system matures, either reduced expression/activity of NKCC1 and/

or increased expression/activity of KCC2 results in low $[Cl^-]_i$ typical of adult neurons (Rivera et al. 1999, 2005; DeFazio et al. 2000; Vardi et al. 2000; Hübner et al. 2001; Stein et al. 2004; Zhang et al. 2007; Delpy et al. 2008; Reynolds et al. 2008; Zhu et al. 2008). GABA can evoke excitatory responses in mature SCN neurons although as described above, the literature is inconsistent regarding: 1) where in the SCN GABA-evoked excitation is generated; and 2) the phase of the circadian cycle in which GABA is excitatory. Some of the differences amongst the studies may be attributed to different recording locations within the SCN which surprisingly are not reported. In that same regard, based on our description of neuron-type specific distribution of KCC2 and KCC4, the general location of recording within the SCN may be less relevant than the specific type of neuron recorded.

Dorsomedial and Ventrolateral SCN Sub-regions and GABA-evoked Excitation

In our study we have intentionally limited the use of the terms dorsomedial and ventrolateral when describing the distribution of cotransporters in the SCN because the cotransporters are not regionally distributed per se but rather they are expressed in a cell-type specific manner. To the extent that specific peptidergic neurons are distributed in a non-homogenous manner, then such is also the case for the cotransporters. Thus, describing KCC2 as found in the ventrolateral SCN would be an oversimplification as would be describing KCC4 as localized to the dorsomedial SCN. If one were sampling these two regions with a recording electrode, cells expressing KCC4 (or VP) would be more likely to be encountered in the dorsomedial SCN and cells expressing KCC2 (or VIP) would be more likely to be encountered in the ventrolateral SCN, but one would still encounter KCC2/VIP neurons in the dorsomedial region and coming across KCC4/VP cells in the ventral SCN would almost seem likely (see Fig. 3). If, as we suggest, the differential expression of KCC2 and KCC4 plays a major role in regulating $[Cl-]_i$, then future studies that describe the specific cell type recorded when examining the excitatory effects of GABA in the SCN may help explain the present inconsistencies. Even without the knowledge of the specific cell type recorded, recent work has suggested that GABA-evoked excitatory responses are more likely to be observed from the dorsal SCN and during the subjective night (Albus et al. 2005;Choi et al. 2008).

Cl^- Cotransporter Regulation

The functional pool of Cl^- cotransporters in neurons is dynamically regulated. Regulation of Cl^- cotransporters on a daily basis in the adult SCN could represent a recapitulation of the developmental process of transcriptional regulation of Cl^- cotransporters. An E-box control element has been identified in the promoter of the KCC2b splice variant (Markkanen et al. 2008). Circadian timing is controlled by interlocked transcriptional feedback loops and DNA binding of the transcription factors CLOCK and BMAL1 has been shown to involve canonical E-box sequences (Takahashi et al. 2008).

Kinases appear to play a major role in the regulation of Cl^- cotransporter functional activity and kinase activity in the SCN could be temporally controlled. Phosphorylation of Cl^- cotransporters appears to be regulated at least in part by the novel serine-threonine kinase WNK that has a unique substitution of cysteine for lysine at a nearly invariant position in the catalytic core (hence with no K [lysine]) (Kahle et al. 2008). Phosphorylation by the WNK3 isoform modulates Cl^- flux by activating NKCC1 while at the same time WNK3-mediated phosphorylation inhibits KCC2; dephosphorylation via phosphatase activity has the opposite effects (Kahle et al. 2005, 2006; del los Heros et al. 2006). In this study we report for the first time that WNK3 protein is localized within the rat SCN. WNK3 mRNA was previously reported in the mouse SCN (Kahle et al. 2005). The WNK1 isoform of the WNK kinase is rhythmically expressed in *Arabidopsis thaliana* and phosphorylates the APRR3 component of the clock-associated APRR1/TOC1 quintet (Murakami-Kojima et al. 2002); the WNK gene

family regulates flowering time in this plant by modulating the photoperiod pathway (Wang et al. 2008).

The results of the present electron microscopic immunocytochemical investigation of WNK3 provide the first evidence for the strong expression of WNK3 kinase in the postsynaptic region of axo-somatic and axo-dendritic synapses on neurons located in the SCN. Moreover, the double-label procedure employing pre-embedding immunoperoxidase labeling with silver/gold substitution for WNK3 and postembedding immunogold staining for GABA, has revealed that most of these synapses are GABAergic. As has been shown previously, the postsynaptic plasma membrane is a region of neurons enriched in $GABA_A$ receptors (Fujiyama et al. 2000; Belenky et al. 2003) which themselves are ligand-gated chloride channels (Kaila, 1994). WNK3 kinase may play an important role in detection of the direction of Cl^- flux in SCN neurons and, thus, in the regulation of the excitability of these cells.

The activity of Cl^- cotransporters is also regulated by protein trafficking, oligomerization, and postsynaptic activity. Increased targeting of KCC2 to the neuronal cell surface via PKC-dependent phosphorylation may play a role in its functional activity (Lee et al. 2007). In addition, activity-dependent regulation has been described for KCC2; downregulation is rapid, consistent with an alteration in membrane trafficking and/or posttranslational modification (Fiumelli and Woodin, 2007; Banke and Gegelashvili, 2008; Hewitt et al. 2009). Coincident pre- and postsynaptic neural activity also has been shown to downregulate NKCC1 (Balena and Woodin, 2008). Moreover, oligomerization of KCC2 and NKCC1 is important for the functional activity of the cotransporters in the neuronal plasma membrane (Blaesse et al. 2006; Parvin et al. 2007).

The cellular mechanism(s) underlying GABA's excitatory action in the SCN is not known with certainty, although regulation of K^+/Cl^- cotransporter activity seems likely to play an important role. The ability of GABA's action to switch from inhibitory to excitatory, perhaps in a cell-type specific manner, may enhance the activity of local sub-circuits within the overall SCN network. Subtle changes in the functional activity of K^+/Cl^- cotransporters can have profound effects on the output of neuronal networks in the hypothalamus (Hewitt et al. 2009). It is clear that a finer level of analysis of SCN neuron interaction is required to fully understand the integrated network capacity of this complex and heterogeneous structure that functions as a biological clock.

Summary

K^+/Cl^- cotransporters are expressed in a cell-specific manner in the SCN and are distributed to different cellular compartments in SCN neurons (Fig. 10). Cl^- flux may be differentially regulated in VIP/GRP neurons expressing KCC2/KCC1 and VP neurons expressing KCC4/KCC3. In addition, Cl^- cotransporters may be dynamically regulated in the SCN. The ability of GABA to evoke excitatory responses in mature SCN neurons may therefore be restricted to a specific neuronal phenotype providing spatial heterogeneity and loosely correlating with a dorsomedial/ventrolateral scheme. Temporal regulation of cotransporter activity to specific phases of the circadian cycle, perhaps via a link to the core transcriptional molecular clock mechanism, may provide an additional level of regulation of GABA's ability to evoke excitatory responses in the SCN.

Acknowledgments

Supported by NIH grants NS035615 (MAB, GEP, PJS), EY017809 (GEP and PJS), DK57708 (DBM), HL077765 (SLA), and a grant from the Israel Science Foundation 1196/07 (YY).

Abbreviations

BSA	bovine serum albumin
$[Cl^-]i$	intracellular chloride concentration
DAB	3,3′-diaminobenzidine tetrahydrochloride
GABA	γ-aminobutyric acid
$GABA_A$	γ-aminobutyric acid receptor A subtype
$>GABA_B$	γ-aminobutyric acid receptor B subtype
GRP	gastrin releasing peptide
IgG	immunoglobulin G
K^+/Cl^-	potassium/chloride
KCC	potassium/chloride cotransporter
$Na^+/K^+/2Cl^-$	sodium/potassium/chloride
NKCC	sodium/potassium/chloride cotransporter
PBS	phosphate buffered saline
PFA	paraformaldehyde
RT	room temperature
SCN	suprachiasmatic nucleus
TBS	tris buffered saline
VIP	vasoactive intestinal peptide
VP	vasopressin
WNK	with no lysine
ZT	zeitgeber time

REFERENCES

Albus H, Vansteensel MJ, Michel S, Block GD, Meijer JH. A GABAergic mechanism is necessary for coupling dissociable ventral and dorsal regional oscillators within the circadian clock. Curr Biol 2005;15:886–893. [PubMed: 15916945]

Aton SJ, Herzog ED. Come together, right …now: synchronization of rhythms in a mammalian circadian clock. Neuron 2005;48:531–534. [PubMed: 16301169]

Aton SJ, Huettner JE, Straume M, Herzog ED. GABA and $G_{i/o}$ differentially control circadian rhythms and synchrony in clock neurons. Proc Natl Acad Sci USA 2006;103:19188–19193. [PubMed: 17138670]

Balena T, Woodin MA. Coincident pre- and postsynaptic activity downregulates NKCC1 to hyperpolarize E_{Cl} during development. Eur J Neurosci 2008;27:2402–2412. [PubMed: 18430034]

Banke TG, Gegelashvili G. Tonic activation of group I mGluRs modulates inhibitory synaptic strength by regulating KCC2 activity. J Physiol 2008;586:4925–4934. [PubMed: 18772206]

Belenky MA, Wagner S, Yarom Y, Matzner H, Cohen S, Castel M. The suprachiasmatic nucleus in stationary organotypic culture. Neuroscience 1996;70:127–143. [PubMed: 8848118]

Belenky MA, Sagiv N, Fritschy JM, Yarom Y. Presynaptic and postsynaptic $GABA_A$ receptors in rat suprachiasmatic nucleus. Neuroscience 2003;118:909–923. [PubMed: 12732237]

Belenky MA, Yarom Y, Pickard GE. Heterogeneous expression of γ-amminobutyric acid and γ-amminobutyric acid-associated receptors and transporters in the rat suprachiasmatic nucleus. J Comp Neurol 2008;506:708–732. [PubMed: 18067149]

Ben-Barak Y, Russel JT, Whitnall MH, Ozata K, Gainer H. Neurophysin in the hypothalamohypophysial system-I. Production and characterization of monoclonal antibodies. J Neurosci 1985;5:81–87. [PubMed: 3880813]

Blaesse P, Guillemin I, Schindler J, Schweizer M, Delpire E, Khiroug L, Friauf E, Nothwang HG. Oligomerization of KCC2 correlates with development of inhibitory neurotransmission. J Neurosci 2006;26:10407–10419. [PubMed: 17035525]

Ben-Ari Y, Gaiarsa J-L, Tyzio R, Khazipov R. GABA: A pioneer transmitter that excites immature neurons and generates primitive oscillations. Physiol Rev 2007;87:1215–1287. [PubMed: 17928584]

Boettger T, Hübner CA, Maier H, Rust MB, Beck FX, Jentsch TJ. Deafness and renal tubular acidosis in mice lacking the K-Cl co-transporter Kcc4. Nature 2002;416:874–878. [PubMed: 11976689]

Boettger T, Rust M, Maier H, Seidenbecher T, Schweizer M, Keating DJ, Faulhaber J, Ehmke H, Pfeffer C, Scheel O, Lemcke B, Horst J, Leuwer R, Pape H-C, Völkl H, Hübner CA, Jentsch TJ. Loss of K-Cl co-transporter KCC3 causes deafness, neurodegeneration and reduced seizure threshold. EMBO J 2003;22:5422–5434. [PubMed: 14532115]

Brown TM, Piggins HD. Electrophysiology of the suprachiasmatic circadian clock. Prog Neurobiol 2007;82:229–255. [PubMed: 17646042]

Castel M, Morris JF. Morphological heterogeneity of the GABAergic network in the suprachiasmatic nucleus, the brain's circadian pacemaker. J Anat 2000;196:1–13. [PubMed: 10697283]

Choi HJ, Lee CJ, Schroeder A, Kim YS, Jung SH, Kim JS, Kim DY, Son EJ, Han HC, Hong SK, Colwell CS, Kim YI. Excitatory actions of GABA in the suprachiasmatic nucleus. J Neurosci 2008;28:5450–5459. [PubMed: 18495878]

Defazio RA, Keros S, Quick MW, Hablitz JJ. Potassium-coupled chloride cotransport controls intracellular chloride in rat neocortical pyramidal neurons. J Neurosci 2000;20:8069–8076. [PubMed: 11050128]

De Jeu MTG, Pennartz CMA. Circadian modulation of GABA function in the rat suprachiasmatic nucleus: excitatory effects during night phase. J Neurophysiol 2002;87:834–844. [PubMed: 11826050]

de los Heros P, Kahle KT, Rinehart J, Bobadilla NA, Vázquez N, Cristobal PS, Mount DB, Lifton RP, Hebert SC, Gamba G. WNK3 bypasses the tonicity requirement for K-Cl cotransporter activation via a phosphatase-dependent pathway. Proc Natl Acad Sci USA 2006;103:1976–1981. [PubMed: 16446421]

Delpy A, Allain A-E, Meyrand P, Branchereau P. NKCC1 cotransporter inactivation underlies embryonic development of chloride-mediated inhibition in mouse spinal motoneuron. J Physiol 2008;586:1059–1075. [PubMed: 18096599]

Fiumelli H, Woodin MA. Role of activity-dependent regulation of neuronal chloride homeostasis in development. Curr Opinion Neurobiol 2007;17:81–86.

Fujiyama F, Fritschy JM, Stephenson FA, Bolam JP. Synaptic localization of GABA(A) receptor subunits in the striatum of the rat. J Comp Neurol 2000;416:158–172. [PubMed: 10581463]

Gao B, Fritschy JM, Moore RY. $GABA_A$-receptor subunit composition in the circadian timing system. Brain Res 1995;700:142–156. [PubMed: 8624705]

Gavrikov KE, Nilson JE, Dmitriev AV, Zucker CL, Mangel SC. Dendritic compartmentalization of chloride cotransporters underlies directional responses of starburst amacrine cells in retina. Proc Natl Acad Sci USA 2006;103:18793–18798. [PubMed: 17124178]

Gribkoff VK, Pieschl RL, Wisialowski TA, Park WK, Strecker GJ, de Jeu MTG, Pennartz CMA, Dudek FE. A reexamination of the role of GABA in the mammalian suprachiasmatic nucleus. J Biol Rhythms 1999;14:126–130. [PubMed: 10194649]

Gribkoff VK, Pieschl RL, Dudek FE. GABA receptor-mediated inhibition of neuronal activity in rat SCN in vitro: pharmacology and influence of circadian phase. J Neurophysiol 2003;90:1438–1448. [PubMed: 12750413]

Gulásci A, Lee CR, Sik A, Viitanen T, Kaila K, Tepper JM, Freund TF. Cell type-specific differences in chloride-regulatory mechanisms and $GABA_A$ receptor-mediated inhibition in rat substantia nigra. J Neurosci 2003;23:8237–8246. [PubMed: 12967985]

Hastings MH, Reddy AB, Maywood ES. A clockwork web: circadian timing in brain and periphery, in health and disease. Nat Rev Neurosci 2003;4:649–661. [PubMed: 12894240]

Hebert SC, Mount DB, Gamba G. Molecular physiology of caution-coupled Cl^- cotransport: the SLC12 family. Eur J Physiol 2004;447:580–593.

Herzog ED. Neurons and networks in daily rhythms. Nat Rev Neurosci 2007;8:790–802. [PubMed: 17882255]

Herzog ED, Aton SJ, Numano R, Sakaki Y, Tei H. Temporal precision in the mammalian circadian system: A reliable clock from less reliable neurons. J Biol Rhythms 2004;19:35–46. [PubMed: 14964702]

Hewitt SA, Wamsteeker JI, Kurz EU, Bains JS. Altered chloride homeostasis removes synaptic constraint of the stress axis. Nat Neurosci 2009;12:438–443. [PubMed: 19252497]

Hodgson AJ, Penke B, Erdei A, Chubb IW, Somogyi P. Antisera to gamma aminobutyric acid – I. Production and characterization using a new model system. J Histochem Cytochem 1985;33:229–239. [PubMed: 3973378]

Hübner CA, Stein V, Hermans-Borgmeyer I, Meyer T, Ballanyi K, Jentsch TJ. Disruption of KCC2 reveals an essential role of K-Cl cotransport already in early synaptic inhibition. Neuron 2001;30:515–524. [PubMed: 11395011]

Kaila K. Ionic basis of $GABA_A$ receptor channel function in the nervous system. Prog Neurobiol 1994;42:489–537. [PubMed: 7522334]

Kahle KT, Rinehart J, de los Heros P, Louvi A, Meade P, Vázquez N, Hebert SC, Gamba G, Gimenez I, Lifton RP. WNK3 modulates transport of Cl^- in and out of cells: Implications for control of cell volume and neuronal excitability. Proc Natl Acad Sci USA 2005;102:16783–16788. [PubMed: 16275911]

Kahle KT, Rinehart J, Ring A, Gimenez I, Gamba G, Hebert SC, Lifton RP. WNK protein kinases modulate cellular Cl_- flux by altering the phosphorylation state of the Na-K-Cl and K-Cl cotransporters. Physiology (Bethesda) 2006;21:326–335. [PubMed: 16990453]

Kahle KT, Ring AM, Lifton RP. Molecular physiology of the WNK kinases. Ann Rev Physiol 2008;70:329–355. [PubMed: 17961084]

Kanaka C, Ohno K, Okabe A, Kuriyama K, Itoh T, Fukuda A, Sato K. The differential expression patterns of messenger RNAs encoding K-Cl cotransporters (KCC1,2) and Na-K-2Cl cotransporter (NKCC1) in the rat nervous system. Neuroscience 2001;104:933–946. [PubMed: 11457581]

Karadsheh MF, Delpire E. Neuronal restrictive silencing element is found in the KCC2 gene: molecular basis for KCC2-specific expression in neurons. J Neurophysiol 2001;85:995–997. [PubMed: 11160529]

Karadsheh MF, Byun N, Mount DB, Delpire E. Localization of the KCC4 potassium-chloride cotransporter in the nervous system. Neuroscience 2004;123:381–391. [PubMed: 14698746]

Khirug S, Yamada J, Afzalov R, Voipio J, Khiroug L, Kaila K. GABAergic depolarization of the axon initial segment in cortical principal neurons is caused by the Na-K-2Cl cotransporter NKCC1. J Neurosci 2008;28:4635–4639. [PubMed: 18448640]

Lee HH, Walker JA, Williams JR, Goodier RJ, Payne JA, Moss SJ. Direct protein kinase C-dependent phosphorylation regulates the cell surface stability and activity of the potassium chloride cotransporter KCC2. J Biol Chem 2007;282:29777–84. [PubMed: 17693402]

Liu C, Reppert SM. GABA synchronizes clock cells within the suprachiasmatic circadian clock. Neuron 2000;25:123–128. [PubMed: 10707977]

Markkanen M, Uvarov P, Airaksinen MS. Role of upstream stimulating factors in the transcriptional regulation of the neuron-specific K-Cl cotransporter KCC2. Brain Res 2008;1236:8–15. [PubMed: 18755167]

Mercado A, Song L, Vazquez N, Mount DB, Gamba G. Functional comparison of the K^+-Cl^- cotransporters KCC1 and KCC4. J Biol Chem 2000;275:30326–30334. [PubMed: 10913127]

Mercado A, Vázquez N, Song L, Cortés Enck AH, Welsh R, Delpire E, Gamba G, Mount DB. NH_2-terminal heterogeneity in the KCC3 K^+-Cl^- cotransporter. Am J Physiol Renal Physiol 2005;289:F1246–F1261. [PubMed: 16048901]

Mercado A, Broumand V, Zandi-Nejad K, Enck AH, Mount DB. A C-terminal domain in KCC2 confers constitutive K^+-Cl^- cotransport. J Biol Chem 2006;281:1016–1026. [PubMed: 16291749]

Moore RY, Speh JC. GABA is the principal neurotransmitter of the circadian system. Neurosci Lett 1993;150:112–116. [PubMed: 8097023]

Murakami-Kojima M, Nakamichi N, Yamashino T, Mizuno T. The APRR3 component of the clock-associated APRR1/TOC1 quintet is phosphorylated by a novel protein kinase belonging to the WNK family, the gene for which is also transcribed rhythmically in *Arabidopsis thaliana*. Plant Cell Physiol 2002;43:675–683. [PubMed: 12091722]

Parvin MN, Gerelsaikhan T, Turner RJ. Regions in the cytosolic C-terminus of the secretory Na(+)-K(+)-2Cl(−) cotransporter NKCC1 are required for its homodimerization. Biochemistry 2007;46:9630–9637. [PubMed: 17655331]

Payne JA, Rivera C, Voipio J, Kaila K. Cation-chloride co-transporters in neuronal communication, development and trauma. Trends Neurosci 2003;26:199–206. [PubMed: 12689771]

Pickard, GE.; Sollars, PJ. The suprachiasmatic nucleus. In: Richard, Masland; Albright, Thomas D., editors. The Senses: A Comprehensive Reference, Volume 1: Vision. Academic Press; San Diego: 2008. p. 537-556.

Pearson MM, Lu J, Mount DB, Delpire E. Localization of the K^+-Cl^- cotransporter, KCC3, in the central and peripheral nervous system: expression in the choroid plexus, large neurons and white matter tracts. Neuroscience 2001;103:481–491. [PubMed: 11246162]

Quintero JE, Kuhlman SJ, McMahon DG. The biological clock nucleus: A multiphasic oscillator network regulated by light. J Neurosci 2003;23:8070–8076. [PubMed: 12954869]

Renno WM. Post-embedding double-gold labeling immunoelectron microscopic co-localization of neurotransmitters in the rat brain. Med Sci Monit 2001;7:188–200. [PubMed: 11257721]

Reynolds A, Brustein E, Liao M, Mercado A, Babilonia E, Mount DB, Drapeau P. Neurogenic role of the depolarizing chloride gradient revealed by global overexpression of KCC2 from the onset of development. J Neurosci 2008;28:1588–1597. [PubMed: 18272680]

Rivera C, Voipio J, Payne JA, Ruusuvuori U, Lahtinen H, Lamsa K, Pirvola U, Saarma M, Kaila K. The K+/Cl− co-transporter KCC2 renders GABA hyperpolarizing during neuronal maturation. Nature 1999;397:251–255. [PubMed: 9930699]

Rivera C, Voipio J, Kaila K. Two developmental switches in GABAergic signaling: the K^+-Cl^- cotransporter KCC2 and carbonic anhydrase CAVII. J Physiol 2005;562:27–36. [PubMed: 15528236]

Roussa E, Shmukler BE, Wilhelm S, Casula S, Stuart-Tilley AK, Thévenod F, Alper SL. Immunolocalization of potassium-chloride cotransporter polypeptides in rat exocrine glands. Histochem Cell Biol 2002;117:335–344. [PubMed: 11976906]

Ivanov TR, Stanley PJ, Baudoin FMH, Chan F, Pinteaux E, Brown PD, Luckman SM. KCC3 and KCC4 expression in rat adult forebrain. Brain Res 2006;1110:39–45. [PubMed: 16872584]

Shimura M, Akaike N, Harata N. Circadian rhythm in intracellular Cl^- activity of acutely dissociated neurons of suprachiasmatic nucleus. Am J Physiol 2002;282:C366–C373.

Shindler KS, Roth KA. Double immunofluorescent staining using two unconjugated primary antisera raised in the same species. J Histochem Cytochem 1996;44:1331–1335. [PubMed: 8918908]

Shirakawa T, Honma S, Katsuno Y, Oguchi H, Honma K. Synchronization of circadian firing rhythms in cultured rat suprachiasmatic neurons. Eur J Neurosci 2000;12:2833–2838. [PubMed: 10971625]

Stein V, Hermans-Borgmeyer I, Jentsch TJ, Hübner CA. Expression of the KCl cotransporter KCC2 parallels neuronal maturation and the emergence of low intracellular chloride. J Comp Neurol 2004;468:57–64. [PubMed: 14648690]

Strecker GJ, Wuarin JP, Dudek FE. $GABA_A$-mediated local synaptic pathways connect neurons in the rat suprachiasmatic nucleus. J Neurophysiol 1997;78:2217–2220. [PubMed: 9325388]

Su W, Shmukler BE, Chernova MN, Stuart-Tilley AK, De Franceschi L, Brugnara C, Alper SL. Mouse K-Cl cotransporter KCC1: cloning, mapping, pathological expression, and functional regulation. Am J Physiol 1999;277:C899–C912. [PubMed: 10564083]

Takahashi JS, Hong H-K, Ko CH, McDearmon EL. The genetics of mammalian circadian order and disorder: implications for physiology and disease. Nat Rev Genetics 2008;9:764–775. [PubMed: 18802415]

van den Pol AN. Gamma-aminobutyrate, gastrin releasing peptide, serotonin, somatostatin and vasopressin: ultrastructural immunocytochemical localization in presynaptic axons in the suprachiasmatic nucleus. Neuroscience 1986;17:643–659. [PubMed: 2422591]

Vardi N, Zhang L, Payne JA, Sterling P. Evidence that different cation chloride cotransporters in retinal neurons allow opposite responses to GABA. J Neurosci 2000;20:7657–7663. [PubMed: 11027226]

Wagner S, Castel M, Gainer H, Yarom Y. GABA in the mammalian suprachiasmatic nucleus and its role in diurnal rhythmicity. Nature 1997;387:598–603. [PubMed: 9177347]

Wagner S, Sagiv N, Yarom Y. GABA-induced current and circadian regulation of chloride in neurons of the rat suprachiasmatic nucleus. J Physiol 2001;537:853–869. [PubMed: 11744760]

Wang Y, Liu K, Liao H, Zhuang C, Ma H, Yan X. The plant WNK gene family and regulation of flowering time in *Arabidopsis*. Plant Biol 2008;10:548–562. [PubMed: 18761494]

Welsh DK, Logothetis DE, Meister M, Reppert SM. Individual neurons dissociated from rat suprachiasmatic nucleus express independently phased circadian firing rhythms. Neuron 1995;14:697–706. [PubMed: 7718233]

Yamaguchi S, Isejima H, Matsuo T, Okura R, Yagita K, Kobayashi M, Okamura H. Synchronization of cellular clocks in the suprachiasmatic nucleus. Science 2003;302:1408–1412. [PubMed: 14631044]

Zhang L, Delpire E, Vardi N. NKCC1 does not accumulate chloride in developing retinal neurons. J Neurophysiol 2007;98:266–277. [PubMed: 17493914]

Zhu L, Polley N, Mathews GC, Delpire E. NKCC1 and KCC2 prevent hyperexcitability in the mouse hippocampus. Epilepsy Res 2008;79:201–212. [PubMed: 18394864]

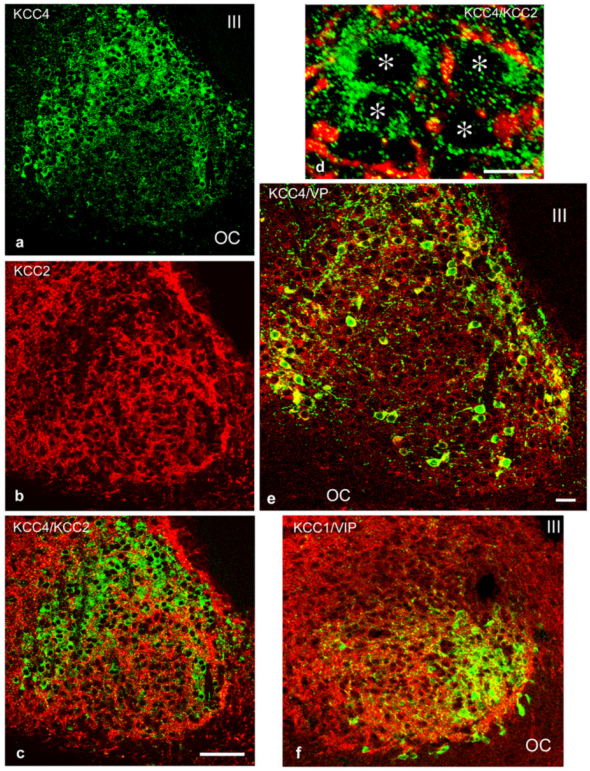

Fig. 1.

Confocal laser microscopy images of sections through the mid-portion of the SCN demonstrating expression of KCC4, KCC2 and KCC1 as well as vasopressin (VP) and vasoactive intestinal peptide (VIP). **a-c:** Images illustrating the expression of KCC4 and KCC2 in different perikarya in the SCN. **d:** High magnification image of a double-labeled SCN section stained for KCC2 (red) and KCC4 (green) illustrating lack of co-expression. KCC4 expressing neurons are marked with asterisks. **e:** A merged confocal image of a 1 μm optical section of the SCN double-labeled with antibodies against KCC4 (red) and vasopressin (VP, green). Note the abundant co-localization of KCC4 immunoreactivity in VP neurons. **f:** A merged confocal image 1 μm optical section through the mid-portion of the SCN double-labeled with antibodies against KCC1 (red) and VIP (green). Note that the pattern of KCC1 expression is very similar to that of KCC2 illustrated in panels **b** and **c**. KCC1 and VIP are co-expressed in many neuronal profiles. Tyramide signal amplification for KCC2 immunoreactivity in **a-d**, and tyramide signal amplification for KCC4 immunoreactivity in **e**. Single optical slices, 1 μm resolution. Scale bar = 25 μm in **a-c** and **f,** 10 μm in **d** and 15 μm in **e**.

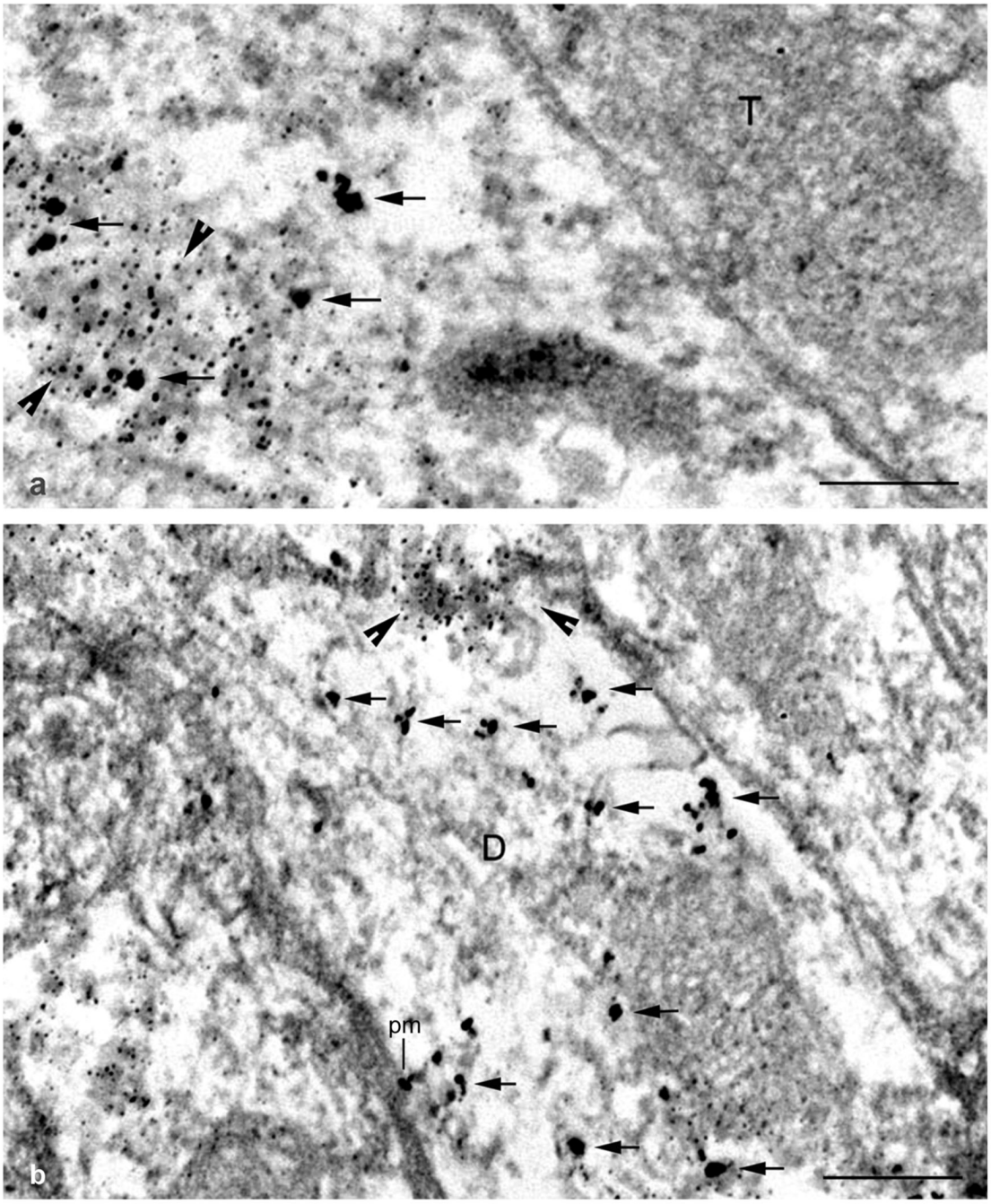

Fig. 2.

Electron micrographs demonstrating co-expression of KCC4 (large gold particles identified with arrows) and NKCC1 (small gold particles pointed out with arrowheads) in a perikaryon (**a**) and a dendritic profile (D in **b**) of SCN neurons from the dorsomedial SCN. Note that KCC4 cotransporter is mainly expressed in the cytoplasm and only single gold particles are associated with the plasma membrane (pm). In panel **b** NKCC1 labeling associated with the plasma membrane is marked with arrowheads. The adjacent nerve terminal (T in panel **a**) is not labeled. Pre-embedding immunogold staining for KCC4 and pre-embedding immunoperoxidase labeling with silver/gold substitution for NKCC1. Tyramide signal amplification for NKCC1. Scale bar = 0.2 μm.

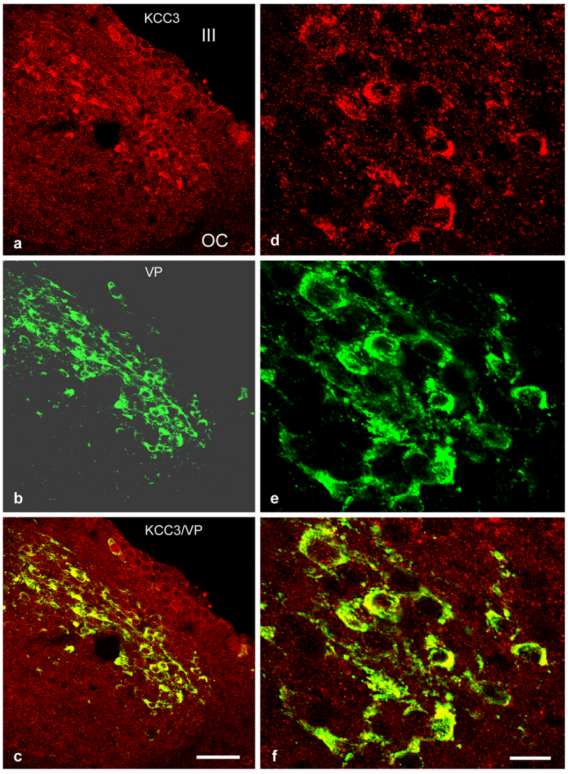

Fig. 3.

Confocal images of the SCN double stained for KCC3 (red; **a**, **d**) and vasopressin (VP, green; **b**, **e**). Note that all neuronal perikarya seen in the merged images (**c**, **f**) co-express KCC3 and vasopressin. KCC3 immunoreactivity is also located in the ependyma lining the third ventricle. For KCC3 antigen retrieval SCN sections were treated with proteinase K followed by incubation in an SDS/mercaptoethanol mixture (see Person et al., 2001 for details). Single optical slices with 1 μm resolution. III, third ventricle; OC, optic chiasm. Scale bar = 25 μm in a-c, and 10 μm in d-f.

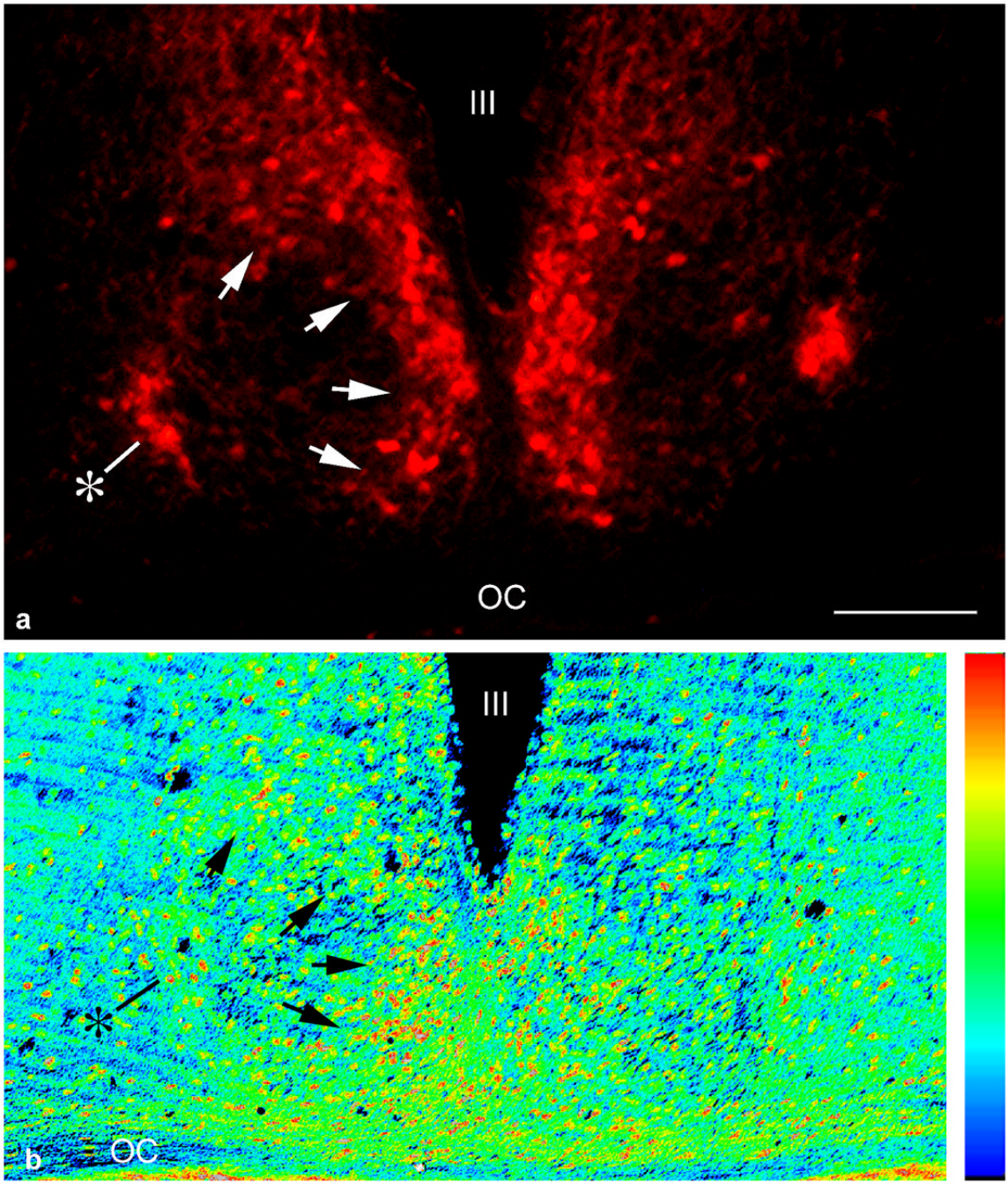

Fig. 4.

Photomicrographs of a section through the mid rostrocaudal region of the SCN double stained with an antibody against vasopressin (panel **a**, immunofluorescent technique with AlexaFluor 594) and rabbit anti-NKCC1 antibody (panel **b**, immunoperoxidase procedure). The latter antibody more clearly detects NKCC1 associated with neuronal perikarya. Image in panel **b** was then pseudocolored to increase the contrast. In animals sacrificed at ZT 5-7 NKCC1 immunoreactivity appears more strongly expressed in the dorsomedial region of the SCN, the region containing the majority of VPergic neurons (arrows). Asterisk shows a group of VP neurons located in the lateral part of the nucleus outside of the high density region of VP neurons. Scale bar = 50 μm.

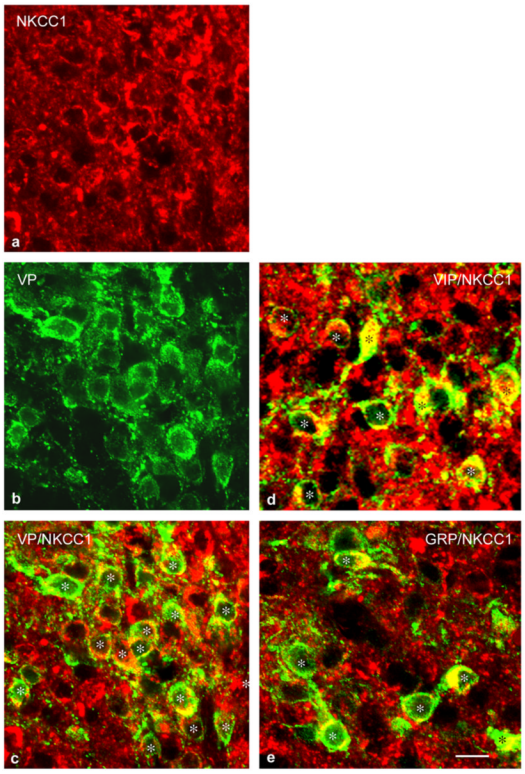

Fig. 5.

Confocal images taken from a mid rostrocaudal region of the SCN of a rat injected with colchicine and immunostained with anti-NKCC1 antibody raised in chicken. Panels **a**-**c** demonstrate coexpression of NKCC1 (red; **a**) and vasopressin (green; **b** and merge in **c**). Merged images in panels **d** and **e** show coexpression of NKCC1 with VIP (**d**) and GRP (**e**), respectively. Asterisks in **c**, **d** and **e** point out the co-labeled neuronal perikarya. Tyramide signal amplification for NKCC1 immunoreactivity. Single optical slices, 1 μm resolution. Scale bar = 10 μm.

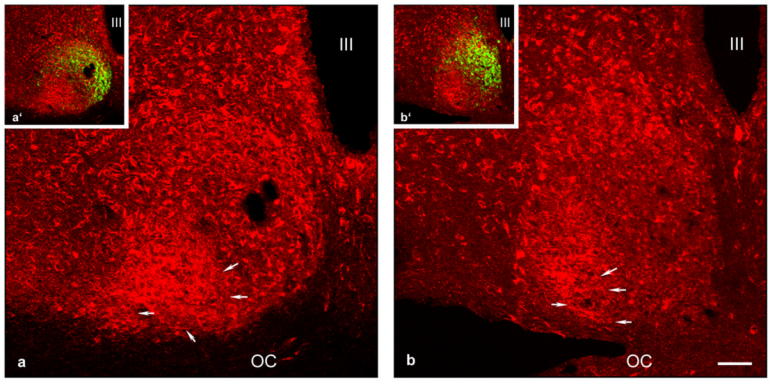

Fig. 6.

Confocal images demonstrating expression of NKCC1 in the mid rostrocaudal region of the SCN from rats sacrificed at ZT5 (panel **a**) and at ZT17 (panel **b**). Small insets at the upper left corner of panels **a** and **b** are merged images captured from the same sections showing the distribution of VP (green in **a′** and **b′**). Note that NKCC1 immunoreactivity is widely expressed in the SCN and in the dorsomedial subregion it is mainly associated with perikarya of neurons containing VP while no robust differences were detected in the staining of these cells in the SCN of rats sacrificed at ZT5 and at ZT17. In the ventral SCN, NKCC1 is not evenly distributed: the medial part of the ventral SCN known to contain intensely stained VIP perikarya shows a low level of NKCC1 immunostaining whereas the lateral part of the same subregion displays abundant, mainly punctuate fluorescence, associated with numerous fibers (arrows). Tyramide signal amplification for NKCC1 immunoreactivity. III, third ventricle; OC, optic chiasm. Scale bar = 25 μm.

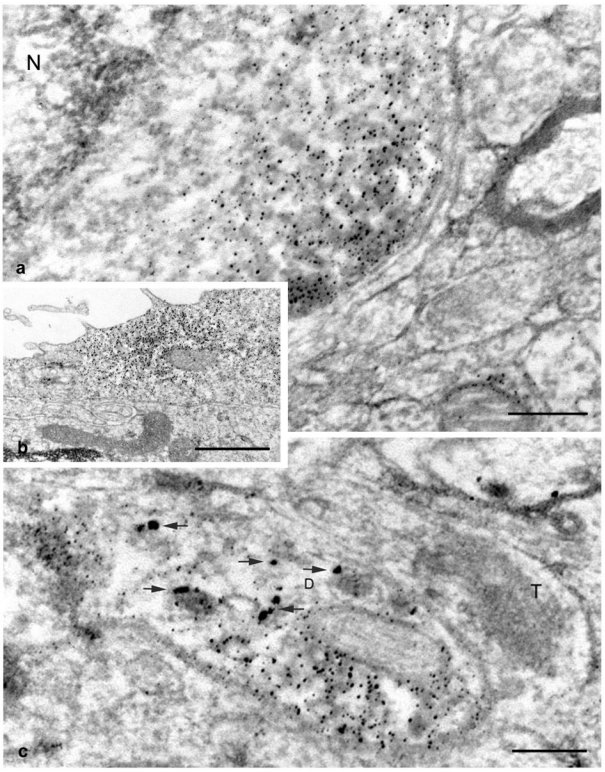

Fig. 7.

Electron micrographs showing distribution of NKCC1in the SCN. **a:** A fragment of a neuron (N) from the ventral SCN with strong labeling near the plasma membrane and in the cytoplasm. **b:** NKCC1 labeling in the apical part of an ependymal cell lining the bottom of the III ventricle. **c:** A dendritic profile (D) from a ample double stained for NKCC1 (small gold particles) and VP (large gold particles). An adjacent nerve terminal (T) is unlabeled. Pre-embedding immunoperoxidase labeling with silver/gold substitution in **a** and **b**, and pre-embedding immunoperoxidase staining with silver/gold substitution for NKCC1 in combination with pre-embedding immunogold labeling for VP in **c**. Tyramide signal amplification for NKCC1 immunoreactivity. Scale bar = 0.2 μm in **a** and **c**, and 0.5 μm in **b**.

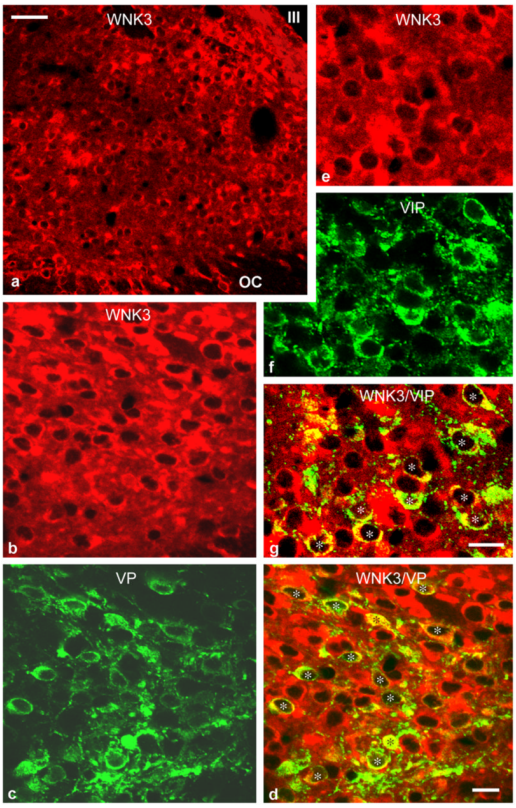

Fig. 8.

Confocal images illustrating the distribution of WNK3, a serine-threonine kinase, in the SCN of a rat subjected to colchicine treatment. (**a**) WNK3 is widely distributed throughout the nucleus although it is more strongly expressed in the dorsomedial subregion. Panels **b**-**d** and **e**-**g** demonstrate expression of WNK3 (red) in VP (green) and VIP (green) SCN neurons, respectively. In panels **d** and **g** neurons co-labeled for WNK3 and either VP (**d**) or VIP (**g**) are marked with asterisks. Tyramide signal amplification for WNK3 immunoreactivity. Single optical slices, 1 μm resolution. III, third ventricle; OC, optic chiasm. Scale bar = 25 μm in a, and 10 μm in b-g.

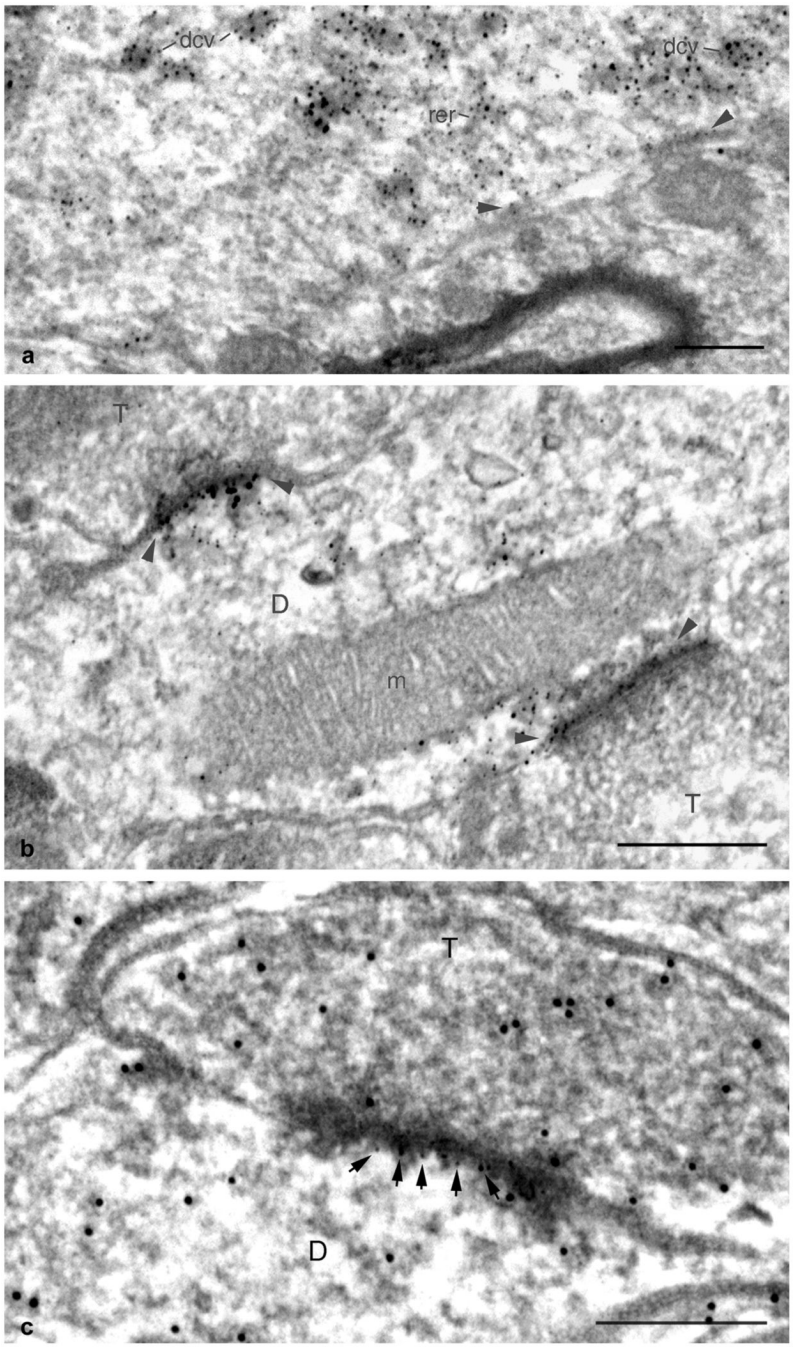

Fig. 9.

Electron micrographs demonstrating sub-cellular distribution of WNK3 kinase in SCN neurons. **a**: Within a perikaryon from the ventral SCN, WNK3 immunoreactivity is associated with the rough endoplasmic reticulum (rer), numerous dense core vesicles (dcv) as well as with the plasma membrane (arrowheads). **b:** Two nerve terminals (T) making contact with a dendrite (D). Note the strong accumulation of WNK3 immunoreactive material near the postsynaptic membrane (arrowheads). **c:** A synapse between a GABAergic (large gold particles) nerve terminal (T) and a GABAergic dendrite (D). Note localized expression of WNK3 immunoreactivity (small gold particles indicated with arrows) near the postsynaptic plasma membrane. Pre-embedding immunoperoxidase labeling with silver/gold substitution for

WNK3 immunoreactivity and postembedding immunogold labeling for GABA. m, mitochondria; Scale bar a-c = 0.2 μm.

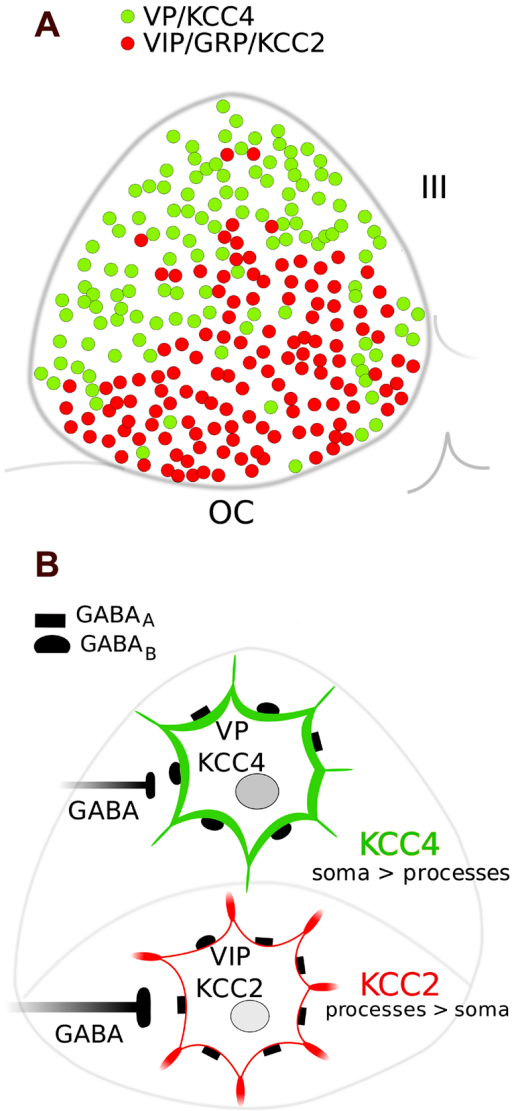

Fig 10.

KCC2 and KCC4 K-Cl cotransporters are expressed in a cell-specific manner in the rat SCN. **A**. Diagrammatic illustration of the neuron-specific distribution of KCC4 (and KCC3) in VP cells and KCC2 (and KCC1) in VIP/GRP cells in the SCN. The distribution of VP/KCC4 cells and VIP/KCC2 cells in the SCN produces a general dorsal/ventral division of the two different K-Cl cotransporters. **B**. Depiction of the VP and VIP/GRP sub-regions of the SCN. GABAergic input is greater to the VIP region compared to the VP region and VIP cells express very few $GABA_B$ receptors whereas VP cells heavily express $GABA_B$ receptors. The subcellular distribution of KCC2 in VIP cells differs from that of KCC4 in VP cells. KCC2 is expressed more heavily in the membrane of dendritic processes of VIP/GRP cells compared to the amount of cotransporter observed in the membrane of the cell soma. KCC4 is more heavily expressed in the membrane of the soma of VP cells compared to the level of KCC4 observed in the membrane of the dendritic processes. VP and VIP/GRP cells express NKCC1 and WNK3 (not shown).

Neuroscience. Author manuscript; available in PMC 2011 February 17.

TABLE 1

Summary of the Primary Antibodies Used in the Present Study[1]

Antiserum	Source	Code	Host	Antigen	Specificity	Dilution
KCC1	Dr. Seth Alper[2]		Rb	C-terminus peptide corresponding to aa 1074-1085 of mouse KCC1coupled to keyhole limpet hemocyanin	By immunoblot and immunofluorescence the AB detects KCC1 while shows minor anti-KCC3, anti-KCC4 and anti-KCC2 activities[2]	1:200
KCC2	Upstate[3]	07-432	Rb	N-terminus peptide corresponding to aa residues 932-1,043 of rat KCC2	By WB the AB recognizes a band at ~140 kDa; absorption with 1 μg of control peptide per 1 ml of diluted AB abolishes the staining	1:7,500 (tyramide enhancing)
KCC3	Dr. David Mount[4]		Rb	KLH-coupled KCC3-specic peptide with aa sequence KKARNAYLNNSNYEEGDEY	By WB the AB recognizes a protein doublet at ~150-170 kDa	1:1,000
KCC4	Dr. David Mount[4]		Rb	KLH-coupled KCC4-specic peptide with aa sequence AERTEEPESPESVDQTSPT	By WB the AB recognizes a band at ~145 kDa	1:1,000
NKCC1	Abcam[6]	Ab37792	Ch	Synthetic peptide corresponding to a sequence located within aa 114-285 of human SLC12A2 (NKCC1)	By WB the AB recognizes a band at ~130 kDa	1:1,500 (tyramide enhancing)
NKCC1	Alpha Diagnostic[7]	NKCC-11A	Rb	C-terminus 22-aa peptide from cytoplasmic domain of rat NKCC1 conjugated to KLH	Specificity of AB was verified by ELISA and AB blocking experiments	15 μg/ml (tyramide enhancing)
WNK3	Abgent[8]	AP7054a	Rb	Synthetic peptide corresponding to a sequence located within aa 1-100 of human WNK3 conjugated to KLH	The AB gives labeling in agreement with other antisera to WNK3; by WB the AB recognizes the control peptide	1:1,500 (tyramide enhancing)
WNK3	Abcam[9]	Ab57690	Ms	Recombinant fragment corresponding to aa 1-101 of human WNK3	The AB gives labeling in agreement with other antisera to WNK3; by WB the AB recognizes the control peptide	1.5 μg/ml (tyramide enhancing)
VP	Dr. Hal Gainer[10]	PS41	Ms	Rat neurophysin-vasopressin conjugated to KLH	By RIA, ELISA and WB recognizes neurophysin-vasopressin; no cross-reactivity with neurophysin-oxytocin	1:10 – 1:50
VIP	Peninsula[11]	T-5030	GP	Human VIP	By RIA no cross-reactivity with PHI-27, PHM-27, VIP(10-28), VIP(1-12), VIP guinea pig and chicken, PACAP-38 and substance P	1:7,500
VIP	DiaSorin[12]	20077	Rb	Porcine VIP	By RIA =0.15% cross-reactivity with PHI, substance P or secretin	1:2,000
GRP	SCBT[13]	SC-7788	Gt	20 aa synthetic peptide mapping within a sequence 1-50 of human GRP conjugated to BSA	The AB gives labeling in agreement with other antisera to GRP; specificity verified by inhibition test using 1 nmol of peptide per ml of diluted AB	1:100 (tyramide enhancing)
GABA	Dr. Peter Somogyi[14]	9	Rb	GABA/BSA conjugate	By ELISA and dot blot analysis no cross-reactivity with Glu, Gln, Gly, Tau, β-Ala, Thr, AABA, Leu	1:2,000

[1] aa, amino acid; AB, antibody; Glu, *l*-glutamate; Gln, *l*-glutamine; Gly, glycine; Tau, taurine; β-Ala, β-alanine; Thr, threonine; Asp, aspartate, Lys, *l*-lysine, Leu, *l*-leucine; AABA, α-aminobutyrate; BABA, β-aminobutyrate; PHI, Peptide Histidine Isoleucine; BSA, bovine serum albumine; KLH, keyhole limpet hemocyanin; Ch, chicken; GP, guinea pig; Gt, goat; Ms, mouse (monoclonal); Rb, rabbit; ELISA, enzyme-linked immunoabsorbent assay; RIA, radioimmunoassay; WB, Western blot.

[2] Su et al., 1999; Roussa et al.,2002

[3] Upstate: Upstate, Lake Plasid, NY; http://www.upstate.com/browse/productdetail.asp?ProductID=07-432

[4] Pearson et al., 2001; Mercado et al., 2005.

[5] Karadsheh et al., 2004

[6] Supplied by Abcam, Cambridge, UK on request; http://www.abcam.com/NKCC1-antibody-Azide-free-ab37792.html

[7] Alpha Diagnostic, San Antonio, TX; http://www.4adi.com/commerce/ccp12344-anti-rat-na-k-cl-cotransporters-1-28nkcc1-bsc229-ig-antibodies-nkcc11-a.htm

[8] Abgent, San Diego, CA; http://www.abgent.com/print/AP7054a

[9] Supplied by Abcam, Cambridge, UK on request; http://www.abcam.com/WNK3-antibody-ab57690.html

[10] Gift from Hal Gainer, NINDS, NIH, Bethesda, MD; Ben-Barak et al.,1985

[11] Peninsula Laboratories Inc, San Carlos CA; http://www.bachem.com

[12] DiaSorin: DiaSorin, Stillwater, MN

[13] Supplied by Santa Cruz Biotechnology, Santa Cruz, CA on request; http://www.scbt.com

[14] Gift from Peter Somogyi, Oxford University, UK; Hodgson et al.,1985